Photoplethysmographic Waveform Versus Heart Rate Variability to Identify Low Stress States. Attention Test

María Dolores Peláez Coca, María Teresa Lozano Albalate, Alberto Hernando Sanz, Montserrat Aiger Vallés, Eduardo Gil.

Abstract—Our long-term goal is the development of an automatic identifier of attentional states. In order to accomplish it, we should firstly be able to identify different states based on physiological signals. So, the first aim of this work is to identify the most appropriate features, to detect a subject high performance state. For that, a database of electrocardiographic (ECG) and photopletysmographic (PPG) signals is recorded in two unequivocally defined states (rest and attention task) from up to 50 subjects as a sample of the population.

Time and frequency parameters of heart/pulse rate variability have been computed from the ECG/PPG signals respectively. Additionally, the respiratory rate has been estimated from both signals and also six morphological parameters from PPG. In total, twenty six features are obtained for each subject. They provide information about the autonomic nervous system and the physiological response of the subject to an attention demand task. Results show an increase of sympathetic activation when the subjects perform the attention test. The amplitude and width of the PPG pulse were more sensitive that the classical sympathetic markers (P_{LFn} and $R_{\text{LF/HF}}$) for identifying this attentional state. State classification accuracy reaches a mean of $89 \pm 2\%$, a maximum of 93% and a minimum of 85%, in the hundred classifications made by only selecting four parameters extracted from the PPG signal (pulse amplitude, pulse width, pulse downward slope and mean pulse rate). These results suggest that attentional states could be identified by PPG.

Index Terms—Photoplethysmographic Waveform, Heart Rate Variability, Low Stress, Bagging.

I. Introduction

There are many professionals, as defence and security personnel, pilots, air traffic controllers, etc, where a high level of attention is necessary to develop their work in safety conditions. This attention may be affected, among others, by psychological stress and by states of sleep deprivation [1], [2]. It is also essential for such personnel to maintain an adequate divided attention, defined as the ability to respond to at least two tasks at the same time [3]. The Brief Test of Attention (BTA) is standardized for the measure of divided attention [4]. Divided attention is a type of simultaneous attention that allows us to process different sources of information and successfully execute more than one task at a time. The BTA

M.D. Peláez, M. Lozano, A. Hernando and M. Aiger are with Centro Universitario de Defensa (CUD), Zaragoza, Spain.

M.D. Peláez, M. Lozano, A. Hernando, and E. Gil are with BSICoS group, Aragón Institute of Engineering Research (I3A), IIS Aragón, University of Zaragoza, Zaragoza, Spain and E. Gil is with Centro de Investigación Biomédica en Red Bioingeniería, Biomateriales y Nanomedicina (CIBER-BBN), Madrid, Spain.

is conceptualized as an auditory perception task that requires divided attention. The two simultaneous requirements of the BTA are simple, with a low level of mental stress [4].

The fundamental hypothesis in which this work is based consists in the fact that alterations in the Autonomic Nervous System (ANS) during the execution of an activity that requires the subject sustained attention can be noninvasively quantified by the recording of physiological signals. These alterations in the ANS can be studied by analysing the Heart Rate Variability (HRV) from the electrocardiographic (ECG) signal or the Pulse Rate Variability (PRV) from the photoplethysmographic (PPG) signal [5]. The ANS is composed by two branches, the sympathetic nervous system and the parasympathetic or vagal nervous system. HRV or PRV spectral analysis reveals two main components: a high-frequency (HF) component, due to respiratory sinus arrhythmia, and a low-frequency (LF) component, which reflects both sympathetic and parasympathetic activity. Power in the HF band has been used as a measure of parasympathetic activity. Normalized power in the LF band and the ratio between power in LF and HF bands have been considered as a measure of sympathovagal balance [6]. Another interesting signal to be considered in ANS analysis is the respiratory signal, which can be extracted from the ECG or PPG signals [7], [8], [9]. Other works found that the breathing pattern is altered during mental stress and attentional tasks [10], [11], [12]. Also, it has been shown that changes in the respiratory pattern alter the spectral content of HRV and PRV [13] and consequently the interpretation of sympathetic or vagal activations [11], [14].

Many studies support that HRV and PRV give similar information about the ANS response [15], [16], [17], [18], [19]. However, PPG recording needs only one low-cost device widely used in the clinical routine that can be located in several parts of the body, while the recording of the ECG signal involves several electrodes all over the chest of the subject, so the PPG signal is more adaptable to the limitations imposed by the different tasks that some professionals must perform.

To the best of our knowledge there are no previous works on identifying attention demand states by means of morphological parameters extracted from the pulse of PPG signal. Changes in the morphology of the PPG signal have been used to detect physical stress [20], the baroreflex response to changes in posture or other forms of blood volume sequestration [21] or even detect mild hypovolemia [22], [23]. Other authors have studied the relationship between systemic vascular re-

sistance and the PPG waveform, specifically with the pulse amplitude, width and slopes [24], finding a high correlation with the first two. An increase in systemic vascular resistance is correlated with an activation of the sympathetic system [25], so the PPG waveform also provides information about the ANS of subjects. In this work, we studied the relationship among attention states and parameters extracted from the PPG waveform, related to the width, amplitude and slope of the pulse.

Knowing the capability of a person to maintain an adequate level of attention at a precise moment is essential before tasks execution where safety is involved. In order to successfully perform this, pattern recognition has various methods of feature selection and classification [26]. In this study, feature selection is done through a wrapping method, that is, a subset of features is selected by considering the accuracy of the classifier. This method allows us to include criteria that avoid redundancy when selecting features. This condition is essential given that HRV and PRV time and frequency features are highly correlated [15], [16], [17], [18], [19]. Including these criteria reduces the number of features that maximize the accuracy of the classifier.

An ensemble learning method is used in this paper. This method facilitates using a set of classifiers so we can obtain greater accuracy compared to using each classifier individually. There are many studies showing improvements in the classification of these methods [27], [28], [29], [30]. There are several techniques that can be used to build these classifier subsets: bootstrap aggregating (bagging), boosting, random subspace and stacking [31]. Among these techniques, bagging obtains the best results when the features of the sample population introduce noise into the classification [32]. In small samples, the classifiers built may be biased and show a large variance in the probability of misclassification. Bagging reduces this error and is usually applied to decision tree methods. Thus, the ensemble learning method selected for the identification of attention demand states in this work is: bagging decision tree method.

The main goal of this study is the automatic identification of a resting state versus an attention demand state. To that end, an analysis of HRV and PRV parameters, together with the respiratory rate extracted from ECG and PPG, and six features extracted from the PPG waveform is done. The use of the PPG waveform parameters to differentiate attentional states is the main innovation of this work.

II. MATERIALS

The generated database includes recordings of 50 subjects (all males). Their mean age is 31 ± 7 years (mean $\pm$ std) and they are mainly military personnel (49 out of 50; 98% of total population).

The ECG and PPG signals are recorded in two unequivocally defined states: rest and attention task. Details of the two registered periods were described below:

- Baseline (*BL*). Subjects remain 5 minutes seated, without performing any task. First 30 seconds from the baseline are discarded. Next 4 minutes are processed, in two segments of two minutes (BL_1 corresponds to the first two minutes; BL_2 corresponds to the last two minutes). In this study, each parameter extracted from the ECG and PPG signals is normalized by the reference state BL_1.

- Attention test (*BTA*). During the attention demand state, subjects perform the BTA which is divided in two parts. In the first one, subjects listen to a recording with 10 lists of letters and numbers with a variable length between 4 and 18 elements, and write how many numbers each list contains, ignoring letters. In the second part, subjects listen to the 10 lists again, but this time they must count letters, ignoring numbers. Two segments of two minutes length of the BTA segment while subjects count numbers (BTA_1), or letters (BTA_2), are processed. These segments are located just 30 seconds after every part of the BTA started.

The recordings were done using the device Nautilus developed by the University of Kaunas, Lithuania [33]. This device allows to record the ECG signal with three leads at a sampling frequency (fs) of 2000 Hz; and the PPG signal (fs = 1000 Hz) in the finger with two possible wavelengths: red and infra-red. The PPG sensor is located in middle finger of the non-dominant hand. Nautilus device also allows recording the ambient temperature (fs = 50 Hz).

III. METHODS

A. Time parameters of HRV and PRV signals

ECG is first down-sampled to 1000 Hz to obtain the same sampling frequency as the PPG signal. A low-pass FIR filter is then applied to both signals to estimate the baseline interference and to remove it from the signal (cut-off frequency of 0.03 Hz and 0.07 Hz for the ECG and PPG signals, respectively) [34]. Another low-pass FIR filter, with cut-off frequency of 35 Hz, is applied over the PPG signal to remove the high frequency noise [8].

Heart beats are detected from the frontal bipolar second lead of the recorded ECG signal using an algorithm based on wavelets [35]. Ectopic beats, missed and false detections are identified and corrected [36]. As a result, QRS complex are located in the ECG and the difference between consecutive R waves conforms the RR time series.

From both wavelength (red and infra-red) of the PPG signal ($x_{\text{PPG}}(n)$), artefactual pulses were suppressed by using the artefact detector described in [37]. Then, the apex (n_{Ai}), the basal (n_{Bi}) and the medium (n_{Mi}) points of the *i-th* PPG pulse were automatically detected using an algorithm based on a low-pass differentiator filter [38]. Fig. 1 shows a PPG signal where its more representative points are highlighted. The medium points are considered the fiducial points in PPG because of their robustness [39], so they are selected to compute the pulse to pulse (PP) time series as the difference between consecutive n_{Mi}.

Five time parameters were computed, from the beat to beat/pulse to pulse time series, as the mean of the two minutes selected for each state (BL_1, BL_2, BTA_1 and BTA_2):

- $\overline{HR}/\overline{PR}$: heart/pulse rate (measure units: s^{-1});

- $\overline{SDNN^{x}}$: standard deviation of all normal-to-normal (NN) intervals (measure units: ms);
- $\overline{SDSD^{x}}$: standard deviation of differences between adjacent NN intervals (measure units: ms);
- $\overline{RMSSD^{x}}$: square root of the mean of the squares of the successive differences between adjacent NN (measure units: ms);
- $\overline{pNN50^{x}}$: number of pairs of successive NN that differ by more than 50 ms, divided by the total number of NN. (measure units: %);

where $x \in [H, P]$ denotes the original signal, ECG or PPG, respectively.
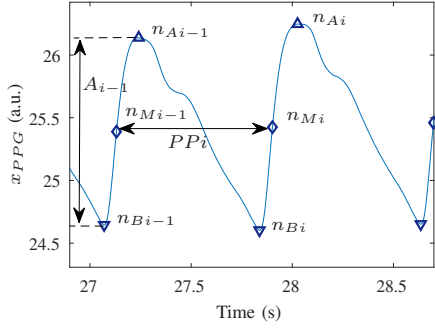
Fig. 1. Pulse waves of the PPG signal (measure in arbitrary units, a.u.) with their most representative points highlighted: the apex (n_{Ai}), the basal (n_{Bi}) and the medium (n_{Mi}) points. Distance between two adjacent medium points is the Pulse to Pulse interval or PPi, used to compute the time series, and distance between the apex and the basal points (A_{i-1}) is the amplitude used to compute the PAV.

B. Frequency parameters of HRV and PRV signals

HRV and PRV frequency analysis are similar: with the beat to beat/pulse to pulse time series, using an algorithm based on the integral pulse frequency modulation model [40], instantaneous heart/pulse rate signal ($d_{XR}(t)$) sampled at 4 Hz is obtained by:

$$d_{XR}(t) = \frac{1 + \mathfrak{m}_{x}(t)}{T_{x}(t)} \quad (1)$$

where $\mathfrak{m}_{x}(t)$ represents the modulating signal which carries the information from ANS and $T_{x}(t)$ is the mean heart/pulse period, which is considered to be slow-time-variant by this model.

Then, a time-varying mean HR or PR, ($d_{XRM}(t)$), is obtained by low-pass filtering $d_{XR}(t)$, with a cut off frequency of 0.03 Hz:

$$d_{XRM}(t) = \frac{1}{T_{x}(t)} \quad (2)$$

Later on, HRV and PRV signals ($d_{XRV}(t)$) are obtained as:

$$d_{XRV}(t) = d_{XR}(t) - d_{XRM}(t) \quad (3)$$

Finally, $\mathfrak{m}_{x}(t)$ is obtained by correcting $d_{XRV}(t)$ by $d_{XRM}(t)$:

$$\mathfrak{m}_{x}(t) = \frac{d_{XRV}(t)}{d_{XRM}(t)} \quad (4)$$

Time-frequency analysis is applied to $\mathfrak{m}_{x}(t)$ to characterize the rapid response of ANS to BTA. The smoothed pseudo Wigner-Ville distribution (SPWVD) is used because it provides better resolution than non-parametric linear methods, independent control of time and frequency filtering, and power is estimated with lower variance than parametric methods when rapid changes occur. The SPWVD of the signal $x(t)$ is defined as [41]:

$$S_x(t, f) = \int \int_{-\infty}^{\infty} \Phi(\tau, \nu) A_x(\tau, \nu) e^{j2\pi(t\nu - \tau f)} d\nu d\tau \quad (5)$$

$$A_x(\tau, \nu) = \int_{-\infty}^{\infty} x\left(t + \frac{\tau}{2}\right) x^*\left(t - \frac{\tau}{2}\right) e^{-j2\nu\pi t} dt \quad (6)$$

where $A_x(\tau, \nu)$ is the narrow band symmetric ambiguity function (AF) of the analytic signal $x(t) = \mathfrak{m}_{x}(t) + j\hat{\mathfrak{m}}_{x}(t)$, where $\hat{\mathfrak{m}}_{x}(t)$ represents the Hilbert transform of $\mathfrak{m}_{x}(t)$. The AF quantifies the time-frequency auto-correlation of $x(t)$ in the delay-doppler frequency domain (τ, ν) and can be seen as the 2D Fourier transform of the Wigner-Ville distribution.

The kernel $\Phi(\tau, \nu)$ was defined as:

$$\Phi(\tau, \nu) = exp\left\{-\pi\left[\left(\frac{\nu}{\nu_0}\right)^2 + \left(\frac{\tau}{\tau_0}\right)^2\right]^{2\lambda}\right\} \quad (7)$$

The iso-contours of $\Phi(\tau, \nu)$ are ellipses whose eccentricity depends on parameters ν_0 and τ_0 [42], [43]. Parameters ν_0 and τ_0 are used to change the length of the ellipses axes aligned along ν (i.e. the degree of time filtering) and τ (i.e. the degree of frequency filtering), respectively. The parameter $\lambda = 0.25$ sets the roll off of the filter. The parameters ν_0 and τ_0 were selected to have a time resolution of 15 s and a frequency resolution of 0.0313 Hz. The time and frequency resolutions were estimated as the full width at half maximum of the SPWVD of a pure sinus and of a temporal impulse, respectively.

For each subject, the temporal evolution of the power content of HRV and PRV within each frequency band, P_B^x was obtained integrating $S_x(t, f)$ in the frequency bands $B \in \{LF, HF\}$.

Finally, four frequency parameters are defined as the mean of the two minutes selected for each state (BL_1, BL_2, BTA_1 and BTA_2):

- $\overline{P_{LF}^x}$: power in the LF band (0.04 - 0.15 Hz; measure units: a.u.);
- $\overline{P_{HF}^x}$: power in the HF band (0.15 - 0.4 Hz; measure units: a.u.);
- $\overline{P_{LF_n}^x}$: power in LF band normalized respect to powers in LF and HF bands (measure units: n.u., normalized units): $\overline{P_{LF_n}^x} = mean(P_{LF}^x(t)/(P_{LF}^x(t) + P_{HF}^x(t)))$;
- $\overline{R_{LF/HF}^x}$: ratio between LF and HF power (measure units: n.u.): $\overline{R_{LF/HF}^x} = mean(P_{LF}^x(t)/P_{HF}^x(t))$.

C. Respiratory information extracted from the ECG and PPG signals

Respiratory signal provides important additional information to complete the ANS analysis. The vagal tone is reflecting

the respiratory sinus arrhythmia, which is synchronous with respiration, so the relationship between respiratory rate and the parasympathetic system must be present in the analysis. Therefore, those subjects with a respiratory rate lower than 0.15 Hz (upper limit of the LF band) or higher than 0.4 Hz (upper limit of the HF band) are discarded to avoid possible misinterpretations in ANS results [11].

Respiratory information can be extracted from ECG or PPG. The first step is to obtain all the derived respiration signals for the ECG (EDR) and the PPG (PDR). Secondly, an algorithm for combining the information of all EDR or all PDR signals is applied in order to estimate a respiratory rate for ECG and PPG respectively.

The method for estimating respiratory rate from the ECG signal presented in [44] is used. It exploits respiration-induced morphology variations in the ECG signal based on 3 EDR signals: upwards to the R-wave slope, downwards to the R-wave slope, and R-wave angle [45]. The method assigns to each beat occurrence the value of its associate QRS slope or R-wave angle. These signals are unevenly sampled, so it is necessary to resample at 4 Hz for standardising them. Finally a mad-based-outlier rejection and a band-pass filter (0.075-1 Hz) are applied. In this study, three leads are registered and three EDR signals are estimated for each lead, so 9 final EDR signals conform the ensemble to extract respiratory information.

When respiratory information is extracted from the PPG signal, the algorithm explained in [8] is applied to the database. In this case the PDR are the PRV, described in section III-B, the Pulse Amplitude Variability (PAV) and the Pulse Width Variability (PWV). An example of these three PDR signals is shown in Fig. 2.

PAV is estimated based on the following equation, using the apex and basal points (n_{Ai} and n_{Bi}) described in section III-A:

$$PAV(n) = \sum_i \left[x_{PPG}(n_{Ai}) - x_{PPG}(n_{Bi}) \right] \delta(n - n_{Ai}) \quad (8)$$

To estimate PWV, firstly start (n_{Oi}) and end (n_{Ei}) points of every pulse in the PPG signal (Fig. 3) have to be identified as in [8]. Then, PWV is defined as:

$$PWV(n) = \sum_i \frac{1}{f_s}(n_{Ei} - n_{Oi})\delta(n - n_{Ai}), \quad (9)$$

where f_s is the sampling rate of the PPG signal.

PAV and PWV signals are unevenly sampled so it is necessary to resample at 4 Hz for standardising them.

The algorithm used to estimate respiratory rate (F_R^x) from the PPG and the ECG signals is the same, only a minor modification in a parameter for the respiratory rate estimation from the PPG signal is necessary due to the low frequency components not related to respiration that appear, changing the peakness conditions and limits as in [7].

Finally, with these two algorithms, a respiratory rate estimation from ECG and PPG is obtained, that allow us to characterise respiratory information in every state.
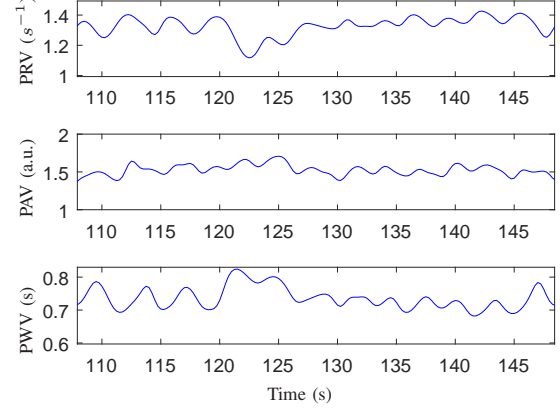

Fig. 2. Example of the PRV, PAV and PWV of a subject of study where the modulation performed by the breathing can be observed.

D. Morphological parameters of PPG signal

The PPG waveform is commonly divided into two phases: the anacrotic phase is the upward segment of the pulses, whereas the catacrotic phase is the downward segment of the pulses. The first phase is primarily concerned with systole, and the second phase with diastole and wave reflections from the periphery [46].

Other authors have studied the relationship between different morphological parameters of the PPG signal with the physiology of subjects [24], [25], [46]. Among the parameters studied, the amplitude and width of the PPG pulses showed a strong correlation with the activation of the sympathetic system [24], [46], although a not so strong relationship was found with the pulse slopes [24].

In this work, six morphological parameters of the PPG signal are considered. The first two are the amplitude (PA) and the width (PW) of the PPG signal, that are estimated based on the following equations, which are similar to the equation in section III-C:

$$PA(i) = x_{PPG}(n_{Ai}) - x_{PPG}(n_{Bi}) \quad (10)$$

$$PW(i) = \frac{1}{f_s}(n_{Ei} - n_{Oi}) \quad (11)$$

The next two parameters are two segments of the PPG wave width. The first segment corresponds to the anacrotic phase of the pulses (PW_u) and the second one to the catacrotic phase (PW_d). The maximum amplitude of the pulse n_{Ai} is the point of separation between them. The parameters are estimated as:

$$PW_u(i) = \frac{1}{f_s}(n_{Ai} - n_{Oi}) \quad (12)$$

$$PW_d(i) = \frac{1}{f_s}(n_{Ei} - n_{Ai}) \quad (13)$$

The last two morphological parameters are defined as the upward and downward slopes of each PPG pulse, simplified as the Pulse Slope (PS). These two parameters are calculated as the ratio between the amplitude and the width of each upward and downward segment, as:

$$PS_u(i) = f_s \frac{x_{PPG}(n_{Ai}) - x_{PPG}(n_{Oi})}{n_{Ai} - n_{Oi}} \qquad (14)$$

$$PS_d(i) = f_s \frac{x_{PPG}(n_{Ai}) - x_{PPG}(n_{Ei})}{n_{Ei} - n_{Ai}} \qquad (15)$$

An outlier identification is carried out on all morphological parameters based on [7], where every sample outside the range $[median \pm G \cdot std]$ of the N_g previous data is removed. In this study $G = 5$ and $N_g = 50$.

In summary, based on the significant points of each PPG pulse (Fig. 3), the following morphological parameters are defined as the mean of the two minutes selected for each state (BL_1, BL_2, BTA_1 and BTA_2):

- $\overline{PW}$. Mean width of the pulses (measure units: s);
- $\overline{PA}$. Mean amplitude of the pulses (measure units: a.u.);
- $\overline{PW_u}$. Mean width of the anacrotic phase of the pulses (measure units: s);
- $\overline{PW_d}$. Mean width of the catacrotic phase of the pulses (measure units: s);
- $\overline{PS_u}$. Mean upward slope of the PPG pulses, calculated as the ratio between amplitude and width of that segment (measure units: a.u.);
- $\overline{PS_d}$. Mean downward slope of the PPG pulses, calculated as the ratio between amplitude and width of that segment (measure units: a.u.).
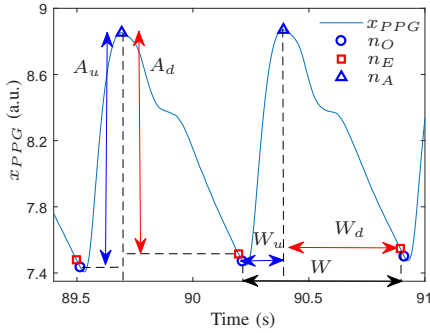
Fig. 3. Location of the start n_{Oi}, the end n_{Ei} and the apex n_{Ai} point, used to calculate the morphological parameters of the PPG signal. Distance between n_{Ai} and n_{Oi} points, in vertical axe, is the amplitude (A_u) and, in horizontal axe, is the width (W_u), both are used to calculate the $\overline{PS_u}$. Distance between n_{Ai} and n_{Ei} points, in vertical axe, is the amplitude (A_d) and, in horizontal axe, is the width (W_d), both are used to calculate $\overline{PS_d}$. Distance between the start and the end points (W) is the width used to compute the $\overline{PW}$.

E. Statistical analysis

A statistical analysis of the 26 parameters obtained from the ECG and the PPG signals was implemented in order to identify both states (rest and attention task). Firstly, an outlier identification for each subject was performed, for this, the following interquartile limits are defined:

$$T_{\mathcal{Y}}^l = Q_2(\mathcal{Y}_{BTA_1}^k - \mathcal{Y}_{BL_1}^k) - 3 \cdot IQR(\mathcal{Y}_{BTA_1}^k - \mathcal{Y}_{BL_1}^k) \qquad (16)$$

$$T_{\mathcal{Y}}^h = Q_2(\mathcal{Y}_{BTA_1}^k - \mathcal{Y}_{BL_1}^k) + 3 \cdot IQR(\mathcal{Y}_{BTA_1}^k - \mathcal{Y}_{BL_1}^k) \qquad (17)$$

The parameters that exceed any of these limits are identified and eliminated of the entire study:

$$\left. \begin{array}{l} \text{If } (\mathcal{Y}_{BTA_1}^k - \mathcal{Y}_{BL_1}^k) < T_{\mathcal{Y}}^l \text{ or} \\ (\mathcal{Y}_{BTA_1}^k - \mathcal{Y}_{BL_1}^k) > T_{\mathcal{Y}}^h \end{array} \right\} \Rightarrow \left\{ \begin{array}{l} \mathcal{Y}_{BTA_1}^k = null \\ \mathcal{Y}_{BTA_2}^k = null \\ \mathcal{Y}_{BL_1}^k = null \\ \mathcal{Y}_{BL_2}^k = null \end{array} \right. \qquad (18)$$

In these equations, $\mathcal{Y}$ is the mean of each one of the 26 parameters in each segment (BTA_1, BTA_2, BL_2 and BL_1) for each subject, and $k = 1...N_k$, where N_k is the number of subjects.

Secondly, every parameter is normalized to the sum of the reference state (BL_1):

$$\mathcal{R}(\mathcal{Y}_S^k) = \frac{\mathcal{Y}_S^k}{\mathcal{Y}_S^k + \mathcal{Y}_{BL_1}^k}, \qquad (19)$$

where S can be BTA_1, BTA_2 or BL_2.

Parameters have been normalized to minimize the effects of the intersubject variance.

Finally, the Shapiro-Wilk test is applied to distinguish whether the parameters have a normal distribution. When the normal distribution of one parameter is verified, the t-Student test is applied. In other case, the Wilcoxon paired test is applied. A p-value$<\alpha$ defines significance, where the significance level α can be 0.05, 0.01 or 0.001. These tests are applied to each one of the 26 normalized parameters extracted from the ECG and PPG signals recorded during the BTA and resting state.

F. Feature selection and classification

Bagging or bootstrap aggregating is a method that generates multiple versions of a predictor and combines them to get a better one [31]. The method consists of the following steps:

1) If $Z = (Z^1, Z^2, ..., Z^n)$ is the training set, a random extraction with replacement is performed, generating N_b subsets: $Z_b = (Z_b^1, Z_b^2, ..., Z_b^n)$ with $b = 1...N_b$. Each subset has the same number of elements as the original set.
2) A simple individual C_b classifier is built with each subset Z_b.
3) The C_b classifiers are combined by selecting the majority class in the final decision rule.

In this study, we resample to entire data set, $N_b = 30$ and $Z^z = \mathcal{R}(\mathcal{Y}_S^k)$ (where $z = 1...n$). A decision tree is selected as simple individual classifier (C_b) in the bagging method. Since bagging ensemble reduces the variance and increases the classification accuracy in classifiers such as decision trees and artificial neural networks [47], [48].

The ensemble classifier obtained with each training set has been validated using leave-one-out cross-validation. That is, one of the subjects, k_{out}, has not been included in the training set, in any of the two states (neither rest or attention task). The classifier is validated with these two states of the subject based on their features ($\mathcal{R}(\mathcal{Y}_S^{k_{out}})$ where possible values for S are BTA_1, BTA_2 and BL_2). The whole process is repeated for $k_{out} = 1...N_k$. In this case, the size of the training set (n) in the bagging method is $2 \cdot (N_k - 1)$. In this equation,

−1 is because one subject is used in the leave-one-out cross-validation and we multiply by 2 because there are two states for each subject.

A wrapping method based on bagging has been used as a feature selector. This feature selection method consists of the following steps:

1) A classifier is trained and validated with each of the features using the leave-one-out method.
2) The feature of the classifier with the greatest accuracy is selected ($F = \{F_1\}$, where F is the set of selected features).
3) A classifier is trained and validated with two features, the one previously selected, in addition to each of the remaining features. The features with redundant information are not considered in this step.
4) The two features of the classifier with the greatest accuracy are selected ($F = \{F_1, F_2\}$).
5) Steps 3 and 4 are repeated, sequentially increasing the number of features ($F = \{F_1, F_2, ...F_f\}$, where f is the maximum number of features that can be selected).

An exclusion criterion for features with redundant information is included in this feature selection process. Other studies have shown that HRV and PRV time and frequency features are highly correlated [15], [16], [17], [18], [19]. Pearsons correlation coefficient is used to corroborate the correlation when both variables have a normal distribution. In other case, the Spearmans coefficient is applied. Consequently, of the features with a high correlation coefficient, only the first one selected will be included in set F. Similarly, only the first respiratory rate selected, estimated from the PPG signal or the ECG signal, will be considered. When imposing these two restrictions, the maximum number of features for the classifier will be 16 (f equal to 16).

The smallest subset with greatest accuracy is selected from these 16 features. Once the most significant features have been selected, the final classifier is trained and validated. Since the results obtained depend on a random subsets generation training process (Z_b), this last step has been repeated 100 times to obtain more reliable accuracy of the final classifier.

A block diagram of this methodology can be seen in Fig. 4.

IV. RESULTS

The population sample used in this study comprises 50 subjects whose ECG and PPG signals are recorded in two states: rest and attention task. Twenty-six parameters are extracted from these signals, 10 from the ECG signal and 16 from the PPG signal. For each of these parameters, the suitability of including each subject is evaluated using two criteria. The first of these criteria is applied to the HRV and PRV frequency parameters. The respiratory rates of nine subjects are lower than 0.15 Hz or greater than 0.4 Hz, which may result in an overestimation of the power in the LF band or an underestimation of the power in the HF band, respectively. Therefore, the frequency parameters of these 9 subjects, extracted from the ECG and PPG signals, are removed from the study. The second criterion is associated with the identification of outliers. For each parameter, the subjects outside the interval

$[T_{\mathcal{Y}}^l \; T_{\mathcal{Y}}^h]$, defined in subsection III-E, are eliminated from the study. The subjects eliminated in each parameter due to this second criterion, and the final population are shown in Tables I and II.

The parameters object of this study can be affected by changes in the ambient temperature of the room where the test is performed. The room temperature sensor indicates that the temperature variations during the recordings were 0 ± 2 degrees Celsius (median $\pm$ iqr).

A. Statistical analysis

Results of the BTAs show a greater number of correct answers when the subjects count letters. The mean correct answers in the population was 8.4 ± 1.1 (mean $\pm$ std) when counting letters and 6.7 ± 1.2 (mean $\pm$ std) when counting numbers, with 10 being the maximum score. This difference in results is significant ($p < 0.001$), as only three subjects obtain better results when counting numbers. However, the number of correct answers maintains a moderate correlation (Spearman's correlation coefficient 0.43) between the two parts of the test.

Table I shows time and frequency parameters obtained from ECG and PPG together with the estimated respiratory rate, for both states and the results of the statistical analysis. These results show a decrease in the power of the HRV and PRV classical bands ($\overline{P_{HF}}$ and $\overline{P_{LF}}$) during both BTA parts. This decrease is significant only in the HF band of the PRV, during BTA_1. In this table the changes produced in HRV and PRV time parameters are shown as significant. These parameters indicate an increase in heart rate when subjects are carrying out the BTA, and a decrease in the other time parameters ($SDNN$, $SDSD$, $RMSSD$ and $pNN50$). These four time parameters are related to the instability of the heart rhythm. A significant increase in the respiratory rate can also be observed during the BTA.

Table II shows the morphological parameters extracted from the PPG signal for both states. This table shows a significant increase in the width of PPG signal pulses when the subjects carry out the BTA, as well as a significant decrease in pulse amplitude during BTA_1. The PPG waveform amplitude is affected by an unknown coefficient that is constant along the recording, which depends on the physiology of each subject. Therefore, normalization of parameters with a baseline reference state is done so that results are not affected by this coefficient. Only the data not affected by this unknown coefficient are shown in Table II.

B. Feature selection and classification

After identifying the parameters that change significantly when the subjects go from a state of rest to carrying out a BTA, this study's next challenge is the automatic identification of these two states. To minimize the effects of the intersubject variance, all parameters are normalized with a $\mathcal{Y}_{BL_1}^k$ reference state. The two classes to be separated correspond to the subjects' resting state ($\mathcal{R}(\mathcal{Y}_{BL_2})$) and an attention demand state ($\mathcal{R}(\mathcal{Y}_{BTA_1})$ and $\mathcal{R}(\mathcal{Y}_{BTA_2})$). The boxplot in Fig. 5 and Fig. 6 show the described ratios of each parameter extracted from the ECG and PPG signals. The boxplot show a large
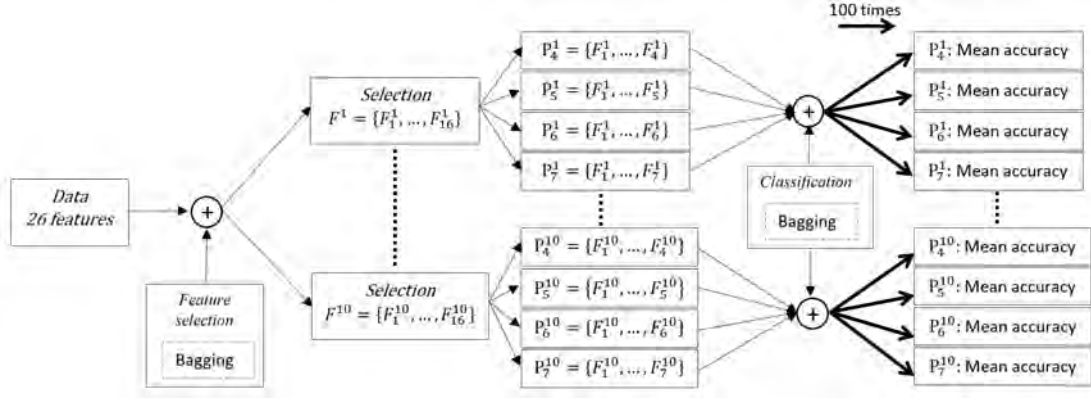
Fig. 4. Selection of features and classification method implemented in this work. The initial data are the normalized values of the states BTA_1 ($\mathcal{R}(\mathcal{Y}_{BTA_1})$) and BL_2 ($\mathcal{R}(\mathcal{Y}_{BL_2})$). P_j^i are subsets of the F^i, which include only the first j features of the F^i selection.

TABLE I

VALUES (MEDIAN ± IQR) OF TIME, FREQUENCY AND RESPIRATION PARAMETERS AT EACH STATE (AU. ARBITRARY UNITS, AD. ADIMENSIONAL, NU. NORMALIZED UNITS) AND THEIR NORMALIZATION. STATISTICAL DIFFERENCES ARE REPRESENTED BY: ⋆ ($p < 0.05$), ⋆⋆ ($p < 0.01$) AND ⋆⋆⋆ ($p < 0.001$). IN THE COLUMNS $\mathcal{R}(\mathcal{Y}_{BTA_1})$ AND $\mathcal{R}(\mathcal{Y}_{BTA_2})$, THE VALUES WITH SUBSCRIPT † INDICATE A NORMAL DISTRIBUTION OF PARAMETERS, IN ALL OTHER CASES THE DISTRIBUTION IS NOT NORMAL. *Final Size* INDICATES FINAL NUMBER OF SUBJECTS USED FOR EACH PARAMETER. (ARBITRARY UNITS: A.U. / NORMALIZED UNITS: N.U.)

Feature		$\mathcal{Y}_{BL_1}$	$\mathcal{Y}_{BTA_1}$	$\mathcal{Y}_{BTA_2}$	$\mathcal{R}(\mathcal{Y}_{BTA_1})$ (n.u.)	$\mathcal{R}(\mathcal{Y}_{BTA_2})$ (n.u.)	Final Size	Outliers
$\overline{P_{\mathrm{LF}}}$ (a.u.)	ECG	4.00 ± 3.69	3.17 ± 3.23	3.71 ± 4.15	0.43 ± 0.30 †	0.52 ± 0.31 †	38	3
	PPG	4.61 ± 5.35	3.71 ± 3.43	3.80 ± 3.04	0.42 ± 0.22 †	0.49 ± 0.32 †	29	12
$\overline{P_{\mathrm{HF}}}$ (a.u.)	ECG	2.47 ± 2.95	1.79 ± 2.14	1.62 ± 2.79	0.46 ± 0.17 †	0.47 ± 0.25 †	35	6
	PPG	3.08 ± 3.01	2.45 ± 2.27	2.71 ± 2.92	0.44 ± 0.13 ⋆⋆	0.49 ± 0.16 †	28	13
$\overline{P_{\mathrm{LFn}}}$ (n.u.)	ECG	0.61 ± 0.32	0.60 ± 0.20	0.61 ± 0.26	0.51 ± 0.09	0.51 ± 0.08	41	0
	PPG	0.56 ± 0.26	0.51 ± 0.27	0.53 ± 0.19	0.49 ± 0.12	0.49 ± 0.14	41	0
$\overline{R_{\mathrm{LF/HF}}}$ (n.u.)	ECG	1.86 ± 2.05	1.62 ± 1.62	1.74 ± 2.08	0.54 ± 0.23 †	0.52 ± 0.21 †	41	0
	PPG	1.52 ± 1.42	1.14 ± 1.39	1.22 ± 0.92	0.47 ± 0.23 †	0.46 ± 0.32 †	41	0
$\overline{HR}$ (s^{-1})	ECG	1.13 ± 0.29	1.20 ± 0.28	1.19 ± 0.28	0.51 ± 0.02 ⋆⋆⋆†	0.51 ± 0.02 ⋆⋆⋆†	50	0
$\overline{PR}$ (s^{-1})	PPG	1.15 ± 0.29	1.25 ± 0.26	1.23 ± 0.32	0.51 ± 0.03 ⋆⋆⋆	0.51 ± 0.02 ⋆⋆⋆	48	2
$\overline{SDNN}$ (ms)	ECG	62.95 ± 34.11	52.54 ± 31.54	59.54 ± 37.11	0.44 ± 0.09 ⋆⋆⋆†	0.44 ± 0.16 ⋆⋆⋆†	50	0
	PPG	67.55 ± 28.35	55.45 ± 35.38	51.75 ± 30.56	0.45 ± 0.10 ⋆⋆⋆†	0.45 ± 0.12 ⋆⋆⋆†	47	3
$\overline{SDSD}$ (ms)	ECG	46.83 ± 36.01	33.82 ± 29.16	37.16 ± 36.08	0.47 ± 0.10 ⋆⋆†	0.46 ± 0.12 ⋆⋆⋆†	48	2
	PPG	50.33 ± 31.98	41.24 ± 27.45	39.47 ± 31.02	0.46 ± 0.08 ⋆⋆†	0.46 ± 0.13 ⋆⋆⋆†	47	3
$\overline{RMSSD}$ (ms)	ECG	46.67 ± 35.91	33.73 ± 29.03	37.03 ± 35.92	0.47 ± 0.10 ⋆⋆†	0.46 ± 0.12 ⋆⋆⋆†	48	2
	PPG	50.17 ± 31.82	39.66 ± 20.58	39.34 ± 30.96	0.46 ± 0.08 ⋆⋆†	0.46 ± 0.13 ⋆⋆⋆†	47	3
$\overline{pNN50}$ (%)	ECG	23.78 ± 33.20	11.96 ± 27.80	10.60 ± 28.20	0.40 ± 0.24 ⋆⋆⋆	0.45 ± 0.35 ⋆⋆⋆	49	1
	PPG	24.09 ± 31.73	15.81 ± 28.62	12.89 ± 24.19	0.43 ± 0.25 ⋆†	0.43 ± 0.28 ⋆⋆†	49	1
$\overline{F_{\mathrm{R}}}$ (Hz)	ECG	0.23 ± 0.09	0.29 ± 0.10	0.28 ± 0.10	0.55 ± 0.05 ⋆⋆⋆†	0.54 ± 0.07 ⋆⋆⋆†	50	0
	PPG	0.22 ± 0.10	0.29 ± 0.10	0.31 ± 0.07	0.55 ± 0.10 ⋆⋆	0.59 ± 0.11 ⋆⋆⋆	50	0

TABLE II

NORMALIZED VALUES (MEDIAN ± IQR) OF MORPHOLOGICAL PARAMETERS OF PPG AT EACH STATE. STATISTICAL DIFFERENCES ARE REPRESENTED BY: ⋆ ($p < 0.05$), ⋆⋆ ($p < 0.01$) AND ⋆⋆⋆ ($p < 0.001$). IN THE COLUMNS $\mathcal{R}(\mathcal{Y}_{BTA_1})$ AND $\mathcal{R}(\mathcal{Y}_{BTA_2})$, THE VALUES WITH SUBSCRIPT † INDICATE A NORMAL DISTRIBUTION OF PARAMETERS, IN ALL OTHER CASES THE DISTRIBUTION IS NOT NORMAL. *Final Size* INDICATES FINAL NUMBER OF SUBJECTS USED FOR EACH PARAMETER.

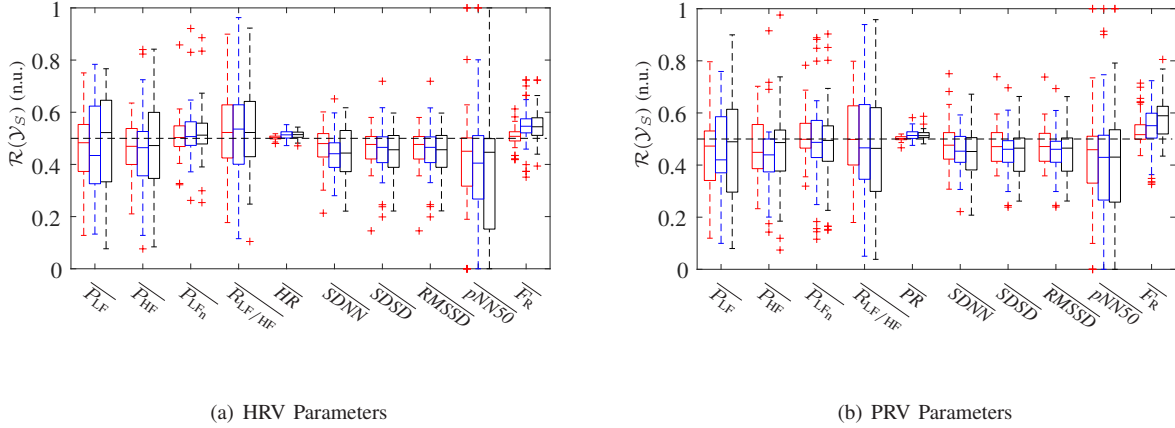| Feature	$\mathcal{R}(\mathcal{Y}_{BTA_1})$(n.u.)	$\mathcal{R}(\mathcal{Y}_{BTA_2})$(n.u.)	Final Size	Outliers
$\overline{PA}$	0.48 ± 0.13 ⋆†	0.50 ± 0.12 †	46	4
$\overline{PW}$	0.52 ± 0.07 ⋆⋆⋆†	0.52 ± 0.08 ⋆†	50	0
$\overline{PW_u}$	0.50 ± 0.01	0.50 ± 0.01	41	9
$\overline{PW_d}$	0.53 ± 0.11 ⋆⋆⋆†	0.54 ± 0.12 ⋆⋆†	50	0
$\overline{PS_u}$	0.48 ± 0.12 ⋆†	0.50 ± 0.13 †	46	4
$\overline{PS_d}$	0.49 ± 0.15 †	0.51 ± 0.15 †	47	3

(a) HRV Parameters

(b) PRV Parameters

Fig. 5. Boxplots of the frequency and time parameters of the HRV and PRV. In red $\mathcal{R}(\mathcal{Y}_{BL_2})$. In blue $\mathcal{R}(\mathcal{Y}_{BTA_1})$. In black $\mathcal{R}(\mathcal{Y}_{BTA_2})$.
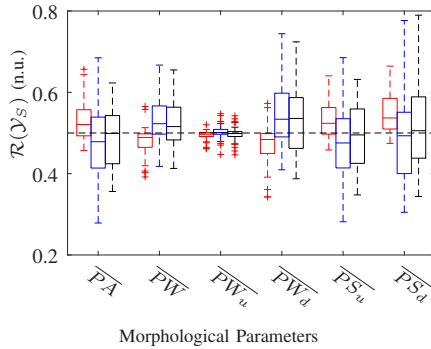

Fig. 6. Boxplots of the morphological parameters extracted from the PPG signal. In red $\mathcal{R}(\mathcal{Y}_{BL_2})$. In blue $\mathcal{R}(\mathcal{Y}_{BTA_1})$. In black $\mathcal{R}(\mathcal{Y}_{BTA_2})$.

dispersion between subjects in HRV and PRV time and frequency parameters ratios than PPG morphological parameters. Moreover, a change in the tendency between $\mathcal{R}(\mathcal{Y}_{BL_2})$ and $\mathcal{R}(\mathcal{Y}_{BTA_1})$ can be observed in this morphological parameters.

Table III shows the correlation coefficient between the HRV and the PRV time and frequency parameters. We can see that this correlation is above 0.57 in almost all the comparisons made. Only in $\overline{P_{LFn}}$ and $\overline{R_{LF/HF}}$, when the BTA is being carried out, does the correlation fall below 0.40. These results indicate that the HRV and the PRV time and frequency parameters are correlated [49]. So that these parameters would provide redundant information in the classification. In order to achieve the greatest possible accuracy, with the least number of features, redundant parameters have not been included in the selection of features.

Finally, the method of feature selection used employs an algorithm based on a bagging ensemble method, requiring a randomness seed, which is why the process is repeated 10 times. Fig. 7.a shows the accuracy obtained in the identification of the $\mathcal{R}(\mathcal{Y}_{BL_2})$ and $\mathcal{R}(\mathcal{Y}_{BTA_1})$ states in each of these 10 processes, by increasing the number of selected features from 1 to 16. Optimal results are those obtained with four, five, six or seven features, due to their great accuracy and their low number of features. For each of the 10 selection cases,

the classification is repeated 100 times with the four, five, six or seven first features. The quality of the results is evaluated with the mean, maximum and minimum accuracy of these 100 repetitions.

Table IV shows the order of the features obtained in the selection process, as well as the accuracy obtained by separating the classes $\mathcal{R}(\mathcal{Y}_{BL_2})$ and $\mathcal{R}(\mathcal{Y}_{BTA_1})$. It shows that the first two features selected in the 10 cases is PPG Pulse Width ($\overline{PW}$) and $\overline{HR}$, or $\overline{PR}$. The following selected features, in each of the cases, are varied without appreciating differences significant in the classification results. However, in five cases, the features three and four are $\overline{P_{LF_n}^P}$ and $\overline{R_{LF/HF}^P}$. Maximum accuracy of 95% is reached in case 4, but with nine features (Fig. 7.a). In Table IV, all cases show a similar accuracy, but in case 4 the first four features are obtained from a single signal, the PPG signal. With these four features and when using the $\mathcal{R}(\mathcal{Y}_{BTA_2})$ and $\mathcal{R}(\mathcal{Y}_{BL_2})$ segments as the test population, average accuracy is $85 \pm 1\%$ (mean $\pm$ std), maximum accuracy is 89% and minimum accuracy is 81%, for 100 repetitions. This validation has been done using the leave-one-out cross-validation method, since the subjects of the training set ($\mathcal{R}(\mathcal{Y}_{BL_2})$ and $\mathcal{R}(\mathcal{Y}_{BTA_1})$) and test set ($\mathcal{R}(\mathcal{Y}_{BL_2})$ and $\mathcal{R}(\mathcal{Y}_{BTA_2})$) are the same.

If feature selection is done only over the parameters extracted form the ECG signal, the maximum accuracy obtained is less than 85% (Fig. 7.b). Similar results are obtained by classifying only with parameters extracted from the PPG signal, excluding the morphological parameters from the feature selection (Fig. 7.c).

V. DISCUSSION

The purpose of this study is the automatic identification of an attention demand state versus a resting state. The resting state corresponds to a state of inactivity, while an attention demand state is induced by a standardized test, the BTA. For this, a database is built with parameters extracted from the ECG and PPG signals of 50 subjects, recorded during those two designated states. HRV and PRV time and frequency parameters are extracted, as well as six morphological parameters from the PPG signal. For an adequate analysis of the frequency

TABLE III
CORRELATION FOR HRV AND PRV PARAMETERS. THE VALUES WITH SUBSCRIPT † CORRESPOND WITH THE PEARSONS CORRELATION COEFFICIENT, IN ALL OTHER CASES THE COEFFICIENTS ARE CALCULATED USING A SPEARMAN RANK CORRELATION.

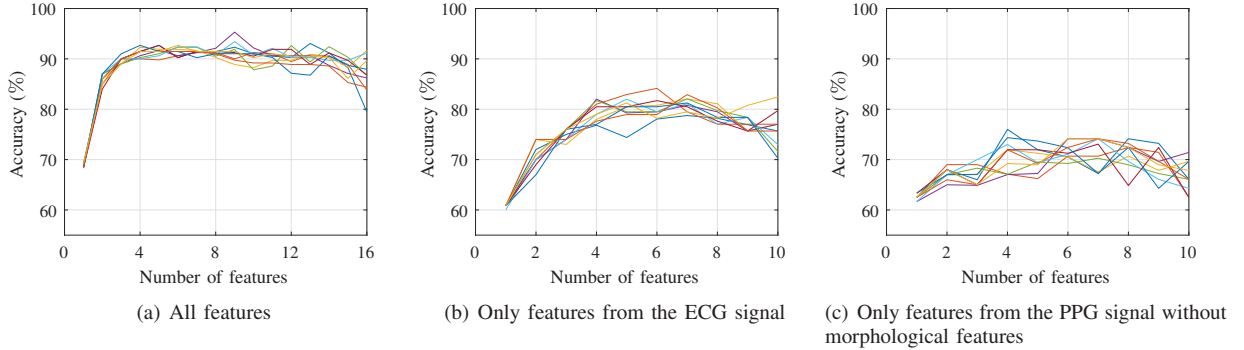|	Parameters	$\overline{P_{\mathrm{LF}}}$	$\overline{P_{\mathrm{HF}}}$	$\overline{P_{\mathrm{LFn}}}$	$\overline{R_{\mathrm{LF/HF}}}$	$\overline{HR/PR}$	$\overline{SDNN}$	$\overline{SDSD}$	$\overline{RMSSD}$	$\overline{pNN50}$
	BL_1	0.57	0.79†	0.67	0.67	0.98†	0.75	0.82	0.82	0.90
Segment	BL_2	0.63	0.93	0.61	0.59	0.99†	0.81	0.83	0.83	0.90
	BTA_1	0.61	0.61†	0.36	0.36	0.95†	0.83†	0.84	0.84	0.87
	BTA_2	0.60	0.61	0.36	0.38	0.95†	0.94	0.88	0.88	0.90

Fig. 7. Accuracy obtained when identifying the subject's state, resting or demand of attention, when the number of selected features increases, in each of the 10 cases generated. (a) All the features have been taken into account in the selection. (b) Only the features extracted from the ECG signal have been considered in the selection. (c) Only the features extracted from the PPG signal, without the morphological feature, have been considered in the selection.

parameters of the HRV and PRV, a recording of the ECG/PPG signals of approximately 2 minutes is necessary [6]. In this work, this constraint has been respected. Likewise, it has been verified that there are no variations in ambient temperature that may affect the parameters under study.

The respiratory rate is extracted from both ECG and PPG signals. This respiratory rate is not only included as a parameter for the development of the classifier, but is also used to complete the subject's ANS response study. To minimize the effect of the intersubject variability, the statistical and classification study is carried out on the proposed parameters ratios, i.e., the states under study are normalized with the subject's baseline state through the equation (19).

One limitation of this work is the non-inclusion of a specific respiratory signal record. To overcome this limitation, two algorithms were implemented to extract the respiratory rate of the ECG and PPG signals [8], [44]. It should be noted that the two algorithms used were tested with respect to a reference device and the good results obtained validate their use for estimating respiratory rates. The margin of error reported for the EDR [44] and PDR [8] methods, in the worst case, has a standard deviation of approximately 0.025 Hz. These algorithms are accurate enough to identify subjects with respiratory rates falling outside the [0.15 Hz 0.4 Hz] band. In this case, these subjects' HRV and PRV frequency parameters are eliminated from the study since they can lead to the ANS response being misinterpreted [11], [14].

Table I shows an increase in respiratory rate and heart rate, together with a significant decrease in the rest of time parameters during the attention demand task. This decrease could suggest that the heart rate of the subjects are more stable during the BTA as these parameters mostly reflect the stability of the signal. Likewise, the F_{R} has been identified in other works with significant differences between stress situations and attentional states versus resting states [11].

Results from the frequency parameters show a significant decrease in the $\overline{P_{\mathrm{HF}}}$ of the PRV, and a non-significant decrease in $\overline{P_{\mathrm{LF}}}$ during the first part of the BTA (BTA_1). Besides, non-significant changes are shown in the normalized values of $\overline{P_{\mathrm{LFn}}}$ and $\overline{R_{\mathrm{LF/HF}}}$. This decrease in the P_{HF} matches with other works where subjects perform high level of attention demanding tasks [11]. In those works, also a significant increase in P_{LFn} and $R_{\mathrm{LF/HF}}$ has been shown. Some authors relate this increase in these sympathetic markers (P_{LFn} and $R_{\mathrm{LF/HF}}$) to the activation of the sympathetic system, which occurs when the subject is exposed to various types of stressors (e.g. mental arithmetic, exams, reaction time) [11], [50]. However, this behaviour is not experimented in our work due to the fact that BTA has a low stress component differently to [11], where the main goal lies in stress generation. On the other hand, other authors question the assertion that $\overline{P_{\mathrm{LFn}}}$ and $\overline{R_{\mathrm{LF/HF}}}$ are a representation of the sympathetic response of the ANS. This assertion is based on four assumptions [51], [52]: (1) cardiac sympathetic nerve activity is a major, if not the exclusive, factor responsible for the LF peak of the heart rate power spectrum; (2) cardiac parasympathetic is exclusively responsible for the HF peak of the heart rate power spectrum; (3) disease or physiological challenges provoke reciprocal changes in cardiac sympathetic and parasympathetic nerve activity; and (4) there is a simple linear interaction between the effects of cardiac sympathetic and cardiac parasympathetic nerve activity on HRV. Each of these statements has been rebutted by several studies [52],

TABLE IV
THE SECOND COLUMN SHOWS THE FIRST SEVEN FEATURES SELECTED IN EACH OF THE 10 CASES. THE FOURTH COLUMN SHOWS THE MEAN AND STANDARD DEVIATION OF THE ACCURACY OBTAINED OF THE ONE HUNDRED REPETITIONS WITH 4, 5, 6 AND 7 FEATURES, WHEN CLASSIFYING THE STATES $\mathcal{R}(\mathcal{Y}_{BL_2})$ AND $\mathcal{R}(\mathcal{Y}_{BTA_1})$. COLUMNS FIVE AND SIX SHOW THE MAXIMUM AND MINIMUM VALUES OF ACCURACY OBTAINED IN THE HUNDRED REPETITIONS OF EACH CLASSIFIER.

Case	Order of feature	Number of feature	mean $\pm$ std (%)	Max (%)	Min (%)
1	$\overline{PW}$; $\overline{HR}$; $\overline{R^P_{\text{LF/HF}}}$; $\overline{P^P_{\text{LF}_\text{n}}}$ $\overline{SDNN^H}$; $\overline{SDSD^H}$; $\overline{pNN50^H}$	4	91 ± 1	93	88
		5	91 ± 1	93	88
		6	89 ± 1	91	85
		7	89 ± 1	90	85
2	$\overline{PW}$; $\overline{HR}$; $\overline{PS_d}$; $\overline{pNN50^H}$ $\overline{P^P_{\text{LF}_\text{n}}}$; $\overline{PS_u}$; $\overline{R^P_{\text{LF/HF}}}$	4	89 ± 1	91	86
		5	88 ± 1	91	85
		6	88 ± 1	91	84
		7	89 ± 1	93	86
3	$\overline{PW}$; $\overline{HR}$; $\overline{P^H_{\text{LF}}}$; $\overline{P^P_{\text{HF}}}$ $\overline{SDSD^P}$; $\overline{pNN50^P}$; $\overline{RMSSD^H}$	4	90 ± 1	92	86
		5	90 ± 1	92	86
		6	90 ± 2	93	85
		7	88 ± 2	92	85
4	$\overline{PW}$; $\overline{PR}$; $\overline{PS_d}$; $\overline{PA}$ $\overline{RMSSD^H}$; $\overline{P^H_{\text{LF}_\text{n}}}$; $\overline{P^H_{\text{LF}}}$	4	89 ± 2	93	85
		5	90 ± 1	93	85
		6	88 ± 2	92	82
		7	89 ± 2	93	85
5	$\overline{PW}$; $\overline{HR}$; $\overline{P^P_{\text{LF}_\text{n}}}$; $\overline{P^H_{\text{LF}}}$ $\overline{P^P_{\text{HF}}}$; $\overline{R^H_{\text{LF/HF}}}$; $\overline{PW_d}$	4	90 ± 1	90	87
		5	90 ± 2	92	86
		6	91 ± 1	92	87
		7	89 ± 2	92	85
6	$\overline{PW}$; $\overline{HR}$; $\overline{PS_d}$; $\overline{SDSD^H}$ $\overline{RMSSD^H}$; $\overline{PA}$; $\overline{P^H_{\text{LF}}}$	4	89 ± 1	91	87
		5	90 ± 1	92	86
		6	90 ± 1	93	86
		7	90 ± 1	92	86
7	$\overline{PW}$; $\overline{HR}$; $\overline{R^P_{\text{LF/HF}}}$; $\overline{P^P_{\text{LF}_\text{n}}}$ $\overline{pNN50^P}$; $\overline{SDNN^H}$; $\overline{PS_d}$	4	91 ± 1	93	88
		5	91 ± 1	93	88
		6	91 ± 1	93	87
		7	90 ± 1	93	88
8	$\overline{PW}$; $\overline{HR}$; $\overline{P^P_{\text{LF}_\text{n}}}$; $\overline{R^P_{\text{LF/HF}}}$ $\overline{pNN50^H}$; $\overline{RMSSD^H}$ $\overline{SDNN^P}$	4	91 ± 1	93	88
		5	91 ± 1	93	87
		6	89 ± 1	91	85
		7	88 ± 1	90	83
9	$\overline{PW}$; $\overline{HR}$; $\overline{R^P_{\text{LF/HF}}}$; $\overline{P^P_{\text{LF}_\text{n}}}$ $\overline{F^H_\text{R}}$; $\overline{pNN50^H}$; $\overline{RMSSD^P}$	4	91 ± 1	93	88
		5	89 ± 2	93	84
		6	89 ± 2	93	87
		7	88 ± 2	91	84
10	$\overline{PW}$; $\overline{HR}$; $\overline{P^P_{\text{LF}_\text{n}}}$; $\overline{R^P_{\text{LF/HF}}}$ $\overline{SDNN^H}$; $\overline{pNN50^H}$; $\overline{F^H_\text{R}}$	4	91 ± 1	93	85
		5	91 ± 1	93	87
		6	91 ± 1	93	88
		7	89 ± 2	93	84

[53]. In particular, the complex nature of LF power and the non-linear interactions between sympathetic and parasympathetic nerve activity, makes it impossible to affirm that the physiological basis of the $\overline{R_{\text{LF/HF}}}$ is due exclusively to the sympathetic branch of the ANS. Similar conclusions can be applied to the interpretation of the $\overline{P_{\text{LFn}}}$.

Concerning morphological PPG parameters, $\overline{PW}$ and $\overline{PW_d}$ values increase when subjects carry out the BTA, being the parameters that reaches the lowest significance level ($\alpha = 0.001$) in their p-value. $\overline{PW_u}$ had no significant changes. These results indicate that there are non-significant changes in systole, and that the change in the width of the pulses are due to changes either in the diastole, or in the wave reflections from the periphery, or in both. Another work showed an increase in the width of PPG signal as the systemic vascular resistance increased, consistent with prolongation of the time required for transmission of the pulse wave at the level of the arteriolar vessels [24]. This increase in systemic vascular

resistance is due to the fact that the innervation of the finger is predominantly adrenergic, that is, it is activated by the sympathetic system [25]. On this basis, the increase of $\overline{PW}$ and $\overline{PW_d}$ observed in our results indicates an activation of the subjects' sympathetic nervous system when carrying out the BTA. However, the classical markers ($\overline{P_{\text{LFn}}}$ and $\overline{R_{\text{LF/HF}}}$) show non-significant changes. Our results also show a significant decrease in $\overline{PA}$ and $\overline{PS_u}$, during the first part of the BTA. The reduction of the $\overline{PA}$ can be attributable either to a loss of central blood pressure or to constriction of the arterioles perfusing the skin. An arterial blood pressure increase due to increased peripheral resistance, as well as a peripheral vasoconstriction, due to an activation of the sympathetic system, could be the respective factors responsible for this reduction in amplitude [46].

During the second part of the BTA (BTA_2), changes in $\overline{P_{\text{HF}}}$, $\overline{PA}$ and $\overline{PS_u}$ cease to be significant, and the remaining parameters stay the same. We also observe that the p value

of $\overline{PW}$ and $\overline{PW_d}$ parameters, during the BTA1 segment, is lower than 0.001, significance level that is not reached during the BTA2 segment. These differences seem to indicate a decrease in the activation of the sympathetic nervous system during the second part of the test, which may be due to a learning curve while carrying out the BTA, or to the fact that counting letters is cognitively simpler for the subjects. The results obtained by the subjects, in each of the BTA parts, supports this observation since the number of correct answers is significantly higher when the subjects count letters.

Other works have suggested that the pulse width, at half height of the beat, correlates with the systemic vascular resistance better than the amplitude [24]. Our results have also obtained a statistical significance in the $\overline{PW}$, corroborating their greater sensitivity to changes in systemic vascular resistance. Additionally, our results show $\overline{PW}$ and $\overline{PA}$ present a higher sensitivity than classical features $\overline{P_{\text{LFn}}}$ and $\overline{R_{\text{LF/HF}}}$ for identifying low sympathetic nervous system activation.

The results obtained from the selection of features corroborate the fact of the great sensitivity of the $\overline{PW}$ for identifying a low sympathetic nervous system activation. The PPG signal width is the first parameter selected in the 10 classification cases shown in Table IV. Fig. 7.a. shows that with this unique feature the classification results approximates 70% of accuracy in these 10 cases. When one more feature is included, the classification accuracy exceeds 80% in all cases. Additionally, the results show that in five cases the features selected in third and fourth position are $\overline{P_{\text{LFn}}}$ and $\overline{R_{\text{LF/HF}}}$, both extracted from the PPG signal. However, the accuracy obtained with the time-frequency features of the PPG signal are very poor if the morphological features of this signal are not included, as can be seen in Fig. 7.c. There are some evidences that the mechanisms of regulation of heart rate and peripheral blood flow are not identical as they could be generated in different central neural structures [54]. These differences could explain the added value of using PPG morphological features for identifying attention states in addition to PRV features.

Similar accuracy is obtained in all cases with four features, but in case 4 these four features are only extracted from the PPG signal: $\overline{PW}$, $\overline{PR}$, $\overline{PS_d}$ and $\overline{PA}$. Except for $\overline{PS_d}$, these features have already been associated with an activation of subjects' sympathetic nervous system by other authors [11], [24], [46]. Table IV shows that the third selected feature, in three of the ten cases, is the downward slope of the PPG pulses ($\overline{PS_d}$). This parameter did not show significant differences between the two studied states; however, it seems to contain relevant information that can assist in automatically identifying the subject's state. These four features accurately identified a different state from a training state. When using the test population $\mathcal{R}(\mathcal{Y}_{BTA_2})$ and $\mathcal{R}(\mathcal{Y}_{BL_2})$, accuracy is maintained at $85 \pm 1\%$ (mean $\pm$ std).

The classification results (Table IV) show that PPG signal morphological parameters are extremely sensitive for the automatic identification of the two studied states: rest and attention task. The significance of PPG signal morphology is for the identification of the subject's state can be clearly seen when, upon applying the same classification algorithm with only features extracted from the ECG or PPG signals, without morphological ones, the accuracy only reaches 85% in the best case (Fig. 7.b and Fig. 7.c). For this reason and based on the results of this study, we can conclude that the PPG signal can differentiate between resting and attention demand states.

VI. CONCLUSION

This study has shown that when subjects carry out a brief attention test they experience a slight activation in their sympathetic nervous system and a lowering of their parasympathetic nervous system ($\overline{P_{\text{HF}}}$ of the PRV. significantly decreases). These results show that PPG pulse width and amplitude ($\overline{PW}$ and $\overline{PA}$) are more sensitive than the classic parameters, $\overline{P_{\text{LFn}}}$ and $\overline{R_{\text{LF/HF}}}$, when detecting the activation of the sympathetic nervous system in mild states of mental stress. They have also shown that parameters extracted from the PPG signal can better identify subjects' resting or attention demand states than parameters extracted from the ECG signal. With only four parameters extracted from the PPG signal ($\overline{PW}$, $\overline{PR}$, $\overline{PS_d}$ and $\overline{PA}$) a mean accuracy of 89% in classification is obtained.

REFERENCES

[1] L. Shin, P. Shin, S. Heckers, and T. Krangel, "Hippocampal function in posttraumatic stress disorder," *Hippocampus*, vol. 14, pp. 292–300., 2004.

[2] M. L. Thomas, H. C. Sing, G. Belenky, H. H. Holcomb, H. S. Mayberg, R. F. Dannals, H. N. Wagner, D. R. Thorne, K. A. Popp, L. M. Rowland, A. B. Welsh, S. M. Balwinski, and D. P. Redmond, "Neural basis of alertness and cognitive performance impairments during sleepiness II. Effects of 48 and 72 h of sleep deprivation on waking human regional brain activity," pp. 199–229, 2003.

[3] D. Kahneman, *Attention and effort.* New York, NY, USA: Prentice-Hall, 1973.

[4] D. Schretlen, J. H. Bobholz, and J. Brandt, "Development and psychometric properties of the brief test of attention," *Clinical Neuropsychologist*, vol. 10, no. 1, pp. 80–89, 1996.

[5] M. Nitzan, A. Babchenko, B. Khanokh, and D. Landau, "The variability of the photoplethysmographic signal - a potential method for the evaluation of the autonomic nervous system," *Physiological Measurement*, vol. 19, no. 1, pp. 93–102, 1998.

[6] Task Force of the European Society of Cardiology the North American Society of Pacing and Electrophysiology, "Heart rate variability standards of measurement, physiological interpretation, and clinical use," *Circulation*, vol. 93, no. 5, pp. 1043–1065, 1996.

[7] R. Bailón, L. Sörnmo, and P. Laguna, "A robust method for ECG-based estimation of the respiratory frequency during stress testing," *IEEE Transactions on Biomedical Engineering*, vol. 53, no. 7, pp. 1273–1285, 2006.

[8] J. Lázaro, E. Gil, R. Bailón, A. Mincholé, and P. Laguna, "Deriving respiration from photoplethysmographic pulse width," *Medical and Biological Engineering and Computing*, vol. 51, no. 1-2, pp. 233–242, 2013.

[9] P. Charlton, D. A. Birrenkott, T. Bonnici, M. A. Pimentel, A. E. Johnson, J. Alastruey, L. Tarassenko, P. J. Watkinson, R. Beale, and D. A. Clifton, "Breathing Rate Estimation from the Electrocardiogram and Photoplethysmogram: A Review," 2017.

[10] D. Widjaja, M. Orini, E. Vlemincx, and S. Van Huffel, "Cardiorespiratory dynamic response to mental stress: A multivariate time-frequency analysis," *Computational and Mathematical Methods in Medicine*, vol. 2013, 2013.

[11] A. Hernando, J. Lazaro, E. Gil, A. Arza Valdes, J. Garzon-Rey, R. Lopez-Anton, C. de la Camara, P. Laguna, J. Aguilo, and R. Bailón, "Inclusion of respiratory frequency information in heart rate variability analysis for stress assessment." *IEEE Journal of Biomedical and Health Informatics*, pp. 1–1, 2016.

[12] E. Vlemincx, J. Taelman, S. De Peuter, I. Van Diest, and O. Van Den Bergh, "Sigh rate and respiratory variability during mental load and sustained attention," *Psychophysiology*, vol. 48, no. 1, pp. 117–120, 2011.

[13] P. Z. Zhang, W. N. Tapp, S. S. Reisman, and B. H. Natelson, "Respiration response curve analysis of heart rate variability," *IEEE Transactions on Biomedical Engineering*, vol. 44, no. 4, pp. 321–325, 1997.

[14] X. Long, P. Fonseca, R. Haakma, R. M. Aarts, and J. Foussier, "Spectral boundary adaptation on heart rate variability for sleep and wake classification," *International Journal on Artificial Intelligence Tools*, vol. 23, no. 03, p. 1460002, 2014.

[15] K. Charlot, J. Cornolo, J. V. Brugniaux, J. P. Richalet, and A. Pichon, "Interchangeability between heart rate and photoplethysmography variabilities during sympathetic stimulations," *Physiological Measurement*, vol. 30, no. 12, pp. 1357–1369, 2009.

[16] E. Gil, M. Orini, R. Bailón, J. M. Vergara, L. Mainardi, and P. Laguna, "Photoplethysmography pulse rate variability as a surrogate measurement of heart rate variability during non-stationary conditions," *Physiological Measurement*, vol. 31, no. 9, pp. 1271–1290, 2010.

[17] S. Lu, H. Zhao, K. Ju, K. Shin, M. Lee, K. Shelley, and K. H. Chon, "Can photoplethysmography variability serve as an alternative approach to obtain heart rate variability information?" *Journal of Clinical Monitoring and Computing*, vol. 22, no. 1, pp. 23–29, 2008.

[18] N. Selvaraj, A. Jaryal, J. Santhosh, K. K. Deepak, and S. Anand, "Assessment of heart rate variability derived from finger-tip photoplethysmography as compared to electrocardiography," *Journal of Medical Engineering and Technology*, vol. 32, no. 6, pp. 479–484, 2008.

[19] A. Hernando, M. Peláez, M. T. Lozano, M. Aiger, D. Izquierdo, A. Sanchez, M. I. Lopez-Jurado, J. I. Moura, J. Fidalgo, J. Lázaro, and E. Gil, "Autonomic nervous system measurement in hyperbaric environments using ECG and PPG signals," *IEEE Journal of Biomedical and Health Informatics*, vol. PP, no. 99, pp. 1–1, 2018.

[20] Y. Li, H. Yan, Z. Xu, M. Wei, B. Zhang, and Z. Shi, "Analysis of the changes in photoplethysmogram induced by exercise stress," *Journal of Medical Imaging and Health Informatics*, vol. 3, no. 3, pp. 347–355, 2013.

[21] S. P. Linder, S. M. Wendelken, E. Wei, and S. P. McGrath, "Using the morphology of photoplethysmogram peaks to detect changes in posture," *Journal of Clinical Monitoring and Computing*, vol. 20, no. 3, pp. 151–158, 2006.

[22] R. Pizov, A. Eden, D. Bystritski, E. Kalina, A. Tamir, and S. Gelman, "Arterial and plethysmographic waveform analysis in anesthetized patients with hypovolemia," *Anesthesiology*, vol. 113, no. 1, pp. 83–91, 2010.

[23] M. Shamir, L. A. Eidelman, Y. Floman, L. Kaplan, and R. Pizov, "Pulse oximetry plethysmographic waveform during changes in blood volume," *British Journal of Anaesthesia*, vol. 82, no. 2, pp. 178–181, 1999.

[24] A. A. Awad, A. S. Haddadin, H. Tantawy, T. M. Badr, R. G. Stout, D. G. Silverman, and K. H. Shelley, "The relationship between the photoplethysmographic waveform and systemic vascular resistance," *Journal of Clinical Monitoring and Computing*, vol. 21, no. 6, pp. 365–372, 2007.

[25] R. E. Klabunde, "Cardiovascular physiology concepts," *Lippincott Williams & Wilkins*, p. 256, 2004.

[26] C. M. Bishop, *Pattern Recognition and Machine Learning*, 2006, vol. 4, no. 4.

[27] A. Mert, N. Kiliç, and A. Akan, "Evaluation of bagging ensemble method with time-domain feature extraction for diagnosing of arrhythmia beats," *Neural Computing and Applications*, vol. 24, no. 2, pp. 317–326, 2014.

[28] E. Bauer, R. Kohavi, P. Chan, S. Stolfo, and D. Wolpert, "An empirical comparison of voting classification algorithms: bagging, boosting, and variants," *Machine Learning*, vol. 36, no. August, pp. 105–139, 1999.

[29] J. Kodovský, J. Fridrich, and V. Holub, "Ensemble classifiers for steganalysis of digital media," in *IEEE Transactions on Information Forensics and Security*, vol. 7, no. 2, 2012, pp. 432–444.

[30] L. K. Hansen and P. Salamon, "Neural network ensembles," *IEEE Transactions on Pattern Analysis and Machine Intelligence*, vol. 12, no. 10, pp. 993–1001, 1990.

[31] L. Breiman, "Bagging predictors," *Machine Learning*, vol. 24, no. 2, pp. 123–140, 1996.

[32] T. G. Dietterich, "An experimental comparison of three methods for constructing ensembles of decision trees: bagging, boosting and ranomization," *Machine Learning*, vol. 40, no. 2, pp. 139–157, 2000.

[33] D. Sokas, M. Gailius, and V. Marozas, "Diver physiology monitor and its graphical user interface," in *Proceedings of International Scientific - Practical Conference, Virtual Instruments in Biomedicine*, 2016, pp. 5–9.

[34] L. Sörnmo and P. Laguna, *Bioelectrical Signal Processing in Cardiac and Neurological Applications*, 2005.

[35] J. P. Martinez, R. Almeida, S. Olmos, A. Rocha, and P. Laguna, "A wavelet-based ECG delineator: evaluation on standard databases," *IEEE Transactions on Biomedical Engineering*, vol. 51, no. 4, pp. 570–581, April 2004.

[36] J. Mateo and P. Laguna, "Analysis of heart rate variability in the presence of ectopic beats using the heart timing signal," *IEEE Transactions on Biomedical Engineering*, vol. 50(3), pp. 334–343, 2003.

[37] E. Gil, J. María Vergara, and P. Laguna, "Detection of decreases in the amplitude fluctuation of pulse photoplethysmography signal as indication of obstructive sleep apnea syndrome in children," *Biomedical Signal Processing and Control*, vol. 3, no. 3, pp. 267–277, 2008.

[38] J. Lázaro, E. Gil, J. M. Vergara, and P. Laguna, "Pulse rate variability analysis for discrimination of sleep-apnea-related decreases in the amplitude fluctuations of pulse photoplethysmographic signal in children," *IEEE Journal of Biomedical and Health Informatics*, vol. 18, no. 1, pp. 240–246, 2014.

[39] J. Y. A. Foo and C. S. Lim, "Pulse transit time as an indirect marker for variations in cardiovascular related reactivity." *Technology and health care : official journal of the European Society for Engineering and Medicine*, vol. 14, pp. 97–108, 2006.

[40] R. Bailón, G. Laouini, C. Grao, M. Orini, P. Laguna, and O. Meste, "The integral pulse frequency modulation model with time-varying threshold: Application to heart rate variability analysis during exercise stress testing," *Biomedical Engineering, IEEE Transactions on*, vol. 58, no. 3, pp. 642–652, March 2011.

[41] W. Martin and P. Flandrin, "Wigner-Ville spectral analysis of nonstationary processes," *IEEE Transactions on Acoustics, Speech, and Signal Processing*, vol. 33, no. 6, pp. 1461–1470, 1985.

[42] M. Orini, R. Bailón, L. T. Mainardi, P. Laguna, and P. Flandrin, "Characterization of dynamic interactions between cardiovascular signals by time-frequency coherence." *IEEE Transactions on Biomedical Engineering*, vol. 59, no. 3, pp. 663–673, Mar 2012.

[43] A. H. Costa and G. F. Boudreaux-Bartels, "Design of time-frequency representations using a multiform, tiltable exponential kernel," *IEEE Transactions on Signal Processing*, vol. 43, no. 10, pp. 2283–2301, 1995.

[44] J. Lázaro, A. Alcaine, D. Romero, E. Gil, P. Laguna, E. Pueyo, and R. Bailón, "Electrocardiogram derived respiratory rate from QRS slopes and R-wave angle," *Annals of Biomedical Engineering*, vol. 40(10), pp. 2072–2083, 2014.

[45] E. Pueyo, L. Sörnmo, and P. Laguna, "QRS slopes for detection and characterization of myocardial ischemia," *IEEE Transactions on Biomedical Engineering*, vol. 55, no. 2, pp. 468–477, 2008.

[46] M. Elgendi, "On the analysis of fingertip photoplethysmogram signals," *Current Cardiology Reviews*, vol. 8, no. 1, pp. 14–25, 2012.

[47] A. R. Webb and K. D. Copsey, *Statistical Pattern Recognition*, 2011, vol. 71, no. 8.

[48] K. Tumer and J. Ghosh, "Error correlation and error reduction in ensemble classifiers," *Connection Science*, vol. 8, no. 3-4, pp. 385–404, 1996.

[49] P. H. Ramsey, "Critical Values for Spearman's Rank Order Correlation," *Journal of Educational and Behavioral Statistics*, vol. 14, no. 3, pp. 245–253, 1989.

[50] G. G. Berntson, J. T. Cacioppo, and A. Fieldstone, "Illusions, arithmetic, and the bidirectional modulation of vagal control of the heart," *Biological Psychology*, vol. 44, pp. 1–17, 1996.

[51] D. L. Eckberg, "Sympathovagal balance: A critical appraisal," pp. 3224–3232, 1997.

[52] G. E. Billman, "The LF/HF ratio does not accurately measure cardiac sympatho-vagal balance," 2013.

[53] D. S. Quintana and J. A. J. Heathers, "Considerations in the assessment of heart rate variability in biobehavioral research," 2014.

[54] V. A. Shvartz, A. S. Karavaev, E. I. Borovkova, S. A. Mironov, V. I. Ponomarenko, M. D. Prokhorov, Y. M. Ishbulatov, E. E. Lapsheva, V. I. Gridnev, and A. R. Kiselev, "Investigation of statistical characteristics of interaction between the low-frequency oscillations in heart rate variability and photoplethysmographic waveform variability in healthy subjects and myocardial infarction patients," *Russian Open Medical Journal*, vol. 5, no. 2, p. e0203, 2016.